Nanoarchitectured 3D cathodes for Li-Ion microbatteries

Manikoth M. Shaijumon, Emilie Perre, Barbara Daffos, Pierre-Louis Taberna, Jean-marie Tarascon, Patrice Simon

Nanoarchitectured 3D Cathodes for Li-Ion Microbatteries

By *Manikoth M. Shaijumon, Emilie Perre, Barbara Daffos, Pierre-Louis Taberna, Jean-Marie Tarascon,* and *Patrice Simon**

Rechargeable lithium ion batteries, due to their high energy density and design flexibility, are the vital power sources for a variety of modern portable electronic devices and are the prime candidates to power next generation of electric vehicles (EVs) and plug-in hybrid electric vehicles (PHEVs).[1] With a rich and versatile chemistry leading to a wide range of electrode materials, several efforts have been devoted to the development of Li-ion technology.[2–5] Apart from the hunt for novel electrode materials to meet high volume applications, newer electrode designs with the existing materials could effectively provide the power necessary to several specific applications. The recent advancements in micro- or nanoelectromechanical systems (MEMS/NEMS) technology have led to a variety of small-scale devices in microelectronics and biomedical area including microsensors, micromachines, and drug delivery systems. Hence the need to develop small-scale electrical power sources that enable on-board microbattery power delivery in these microscale devices. Insufficient power from 2D microbattery configurations leads to the search for development of 3D micro- or nanobattery using cheap and light micro/nano fabrication materials.[6] Such battery designs are expected to offer marked improvements in power while maintaining comparable energy density as compared to 2D. Several configurations have been recently proposed for 3D Li-ion microbatteries to meet the required energy and power densities.[6] Standard depositions of electrode and electrolyte layers onto nanostructured current collectors are seen as an efficient and feasible route for the fabrication of 3D microbatteries. We have previously shown that free standing arrays of copper and aluminium nanorods can be directly grown on the respective base substrates using template approach.[4,7] However, there are only a few reports on 3D microbatteries and most of them have been largely devoted to 3D negative electrodes.[8–11] Nanostructured 3D negative electrodes show improved capacities and rate capabilities compared to their planar counterparts.[8] It is now important to develop 3D positive electrodes to facilitate the 3D microbattery cell assembly, and there have not been any reports on Li-based 3D cathodes in the literature. Here, we show for the first time the design and making of nanoarchitectured 3D positive electrode for lithium ion microbattery applications. For lithium ion batteries, $LiCoO_2$ is the most commonly used cathode material, due to its high capacity and good cyclability.[1,12,13] $LiCoO_2$ is chosen in the present work based on its simple fabrication process to obtain nanostructured deposits using sol-gel route. Standard and uniform deposition of $LiCoO_2$ has been achieved by thermal decomposition of sol-gel precursors spray-coated onto 3D Al nanorod current collectors directly grown on Al substrates. The microstructure and surface morphology of 3D cathodes are characterized by X-ray diffraction (XRD), field emission scanning electron microscopy (FESEM), and transmission electron microscopy (TEM). Detailed studies on the electrochemical behaviour of 3D positive electrodes for lithium ion microbattery applications are reported.

Vertical arrays of Al nanorods were directly grown onto Al foil by pulsed-potential electrodeposition technique, as previously reported.[7] Pulsed deposition technique using clamped stack cell design[4] ensures better electrolyte feed into the pore of alumina membrane, leading to uniform deposition of aluminium. Potential pulses applied for 1 h resulted in uniform growth of Al nanorods with diameters of 200 nm (defined by the pore size of alumina membrane used) and a uniform height of ≈8 μm with a good adherence to the substrate. The obtained Al nanorods maintain the interspace between nanorods arrays (**Figure 1a**) and thus could be used for the standard deposition of positive electrode materials/electrolyte towards the making of 3D microbattery devices. In addition, these 3D current collectors increase the active surface area, while maintaining the small footprint area of the battery, which is one of the major goals of the work.

The positive electrode material $LiCoO_2$ was deposited by thermal decomposition of sol-gel precursors evenly spray-coated onto Al nanorods. Conformal deposition of $LiCoO_2$ has been achieved (Figure 1b–d) with uniform thickness, with an annealing temperature of 650 °C. Energy dispersive X-ray spectroscopy (EDX) analysis revealed the presence of Co and O along with Al, the current collector (Figure 1d). The presence of Li could not be detected using the EDX technique. The process of spray-coating and annealing was repeated 2 to 5 times to obtain the wanted coating of $LiCoO_2$ deposit. We observed that three layers of $LiCoO_2$ deposition resulted in standard coating of 3D Al nanorod current collectors (30 nm thick), maintaining an adequate interspace between the electrode arrays for sequential deposition of subsequent electrolyte and the anode material (Figure 1c, inset: Figure 1d). Thicker layers (>3) have resulted in filling the interspace between the electrode arrays (not shown). Throughout the work, we used 3 layers deposit of $LiCoO_2$ onto Al nanorods for the electrochemical testing of 3D cathodes. **Figure 2a**

[*] Dr. M. M. Shaijumon,[+] Dr. E. Perre, B. Daffos, Dr. P.-L. Taberna, Prof. P. Simon
CIRIMAT, UMR CNRS 5085
Université Paul Sabatier
118 route de Narbonne, 31062 Toulouse Cedex 9 (France)
E-mail: simon@chimie.ups-tlse.fr
Prof. J.-M. Tarascon
LRCS UMR CNRS 6007
Université de Picardie Jules Verne
33 rue Saint Leu, 80039 Amiens (France)
[+] Present address: School of Physics, Indian Institute of Science Education and Research Thiruvananthapuram, Kerala, (India) 695016

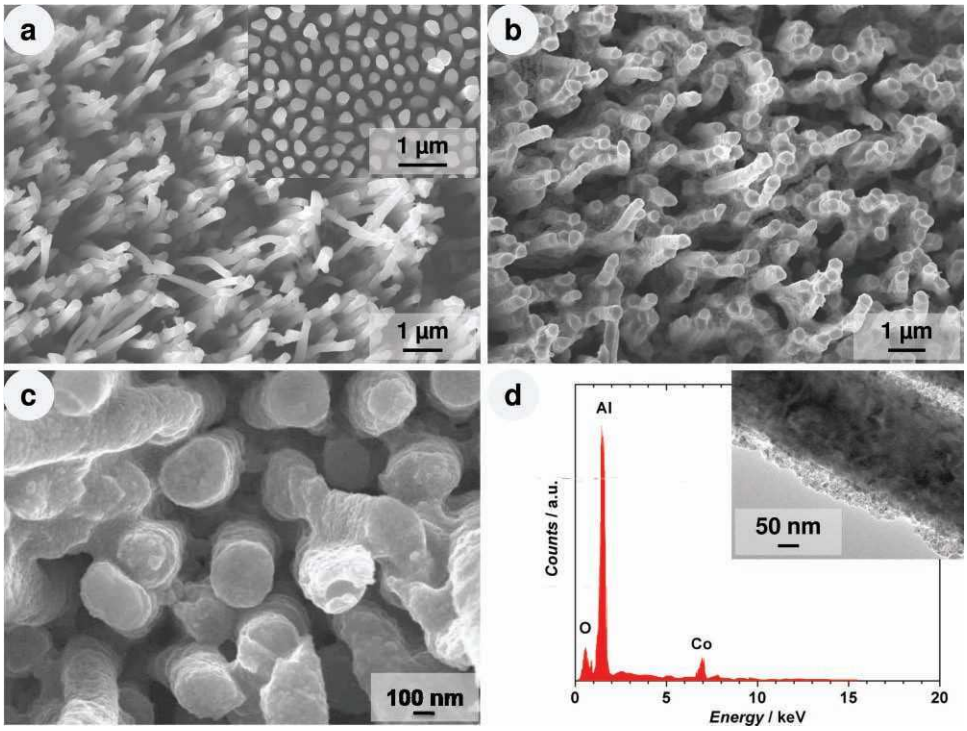

Figure 1. a) SEM image of aluminium nanorods directly grown on Al substrate: inset shows a top view. b) Low and c) high magnification SEM images of Al nanorod-supported $LiCoO_2$ deposits. d) EDX pattern of Al nanorod-supported $LiCoO_2$ deposits. Inset shows a cross-sectional high magnification TEM image of Al nanorod-supported $LiCoO_2$ deposits.

shows the XRD patterns of Al nanorods-supported $LiCoO_2$ electrode. For comparison, XRD patterns of as-prepared bulk $LiCoO_2$ powder and that of aluminium nanorods substrate are shown in Figure 2b,c, respectively. XRD patterns (Figure 2a,b) match well the standard values of $LiCoO_2$ (ICDD card no. 44–0145) and show good crystallization with an annealing temperature of 650 °C. Unit cell parameters of a = 2.810 Å and c = 14.196 Å were calculated from the XRD pattern, which are in good agreement with the literature values of 2.817 Å and 14.037 Å respectively.[14] Two very low intensity extra peaks observed in XRD pattern at 31.2° and 36.8° were matching well with the Co_3O_4 phase (ICDD card no. 042–1467). It was reported that nanostructured $LiCoO_2$ in the shape of nanofibres and nanotubes with good crystallinity could be grown at annealing temperatures of 500–700 °C .[14,15] We have studied different annealing temperatures for growing $LiCoO_2$ and a high degree of crystallinity has been observed at 650 °C, as indicated in the XRD patterns. At this point, it should be recalled that Ceder et al. have identified new cathode materials in which non-transition metals are substituted for cobalt.[16] $LiCo_{1-x}Al_xO_2$ phases have been reported and an increase in cell voltage with Al substitution has been experimentally verified.[16] It is interesting to note that such a partial substitution does not occur here. This could be due to the fact that the heating temperature in the present work is quite lower than one used in reference 16 and that Al-doped precursors have been used for the preparation of $LiCo_{1-x}Al_xO_2$ samples.[16]

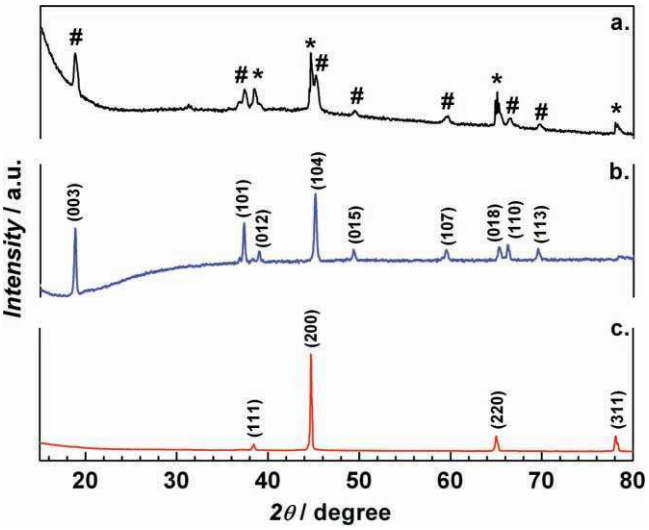

Figure 2. X-ray diffraction patterns (Cu Kα radiation) of a) Al nanorod-supported $LiCoO_2$ electrode, b) $LiCoO_2$ bulk powder, and c) 3D aluminium nanorods current collector.

The Al nanorods-supported $LiCoO_2$ electrodes were used as cathodes in Li half cells which were cycled in a galvanostatic mode with a charge cutoff voltage of 4.15 V. The first 10 cycles of charge–discharge curves for Al nanorods-supported $LiCoO_2$ 3D electrode cycled at a rate of $C/10$ versus Li (**Figure 3a**) show a flattening plateau around 3.9 V, which is typical of the layered $LiCoO_2$ phase, which corresponds to the first-order phase transition between two hexagonal phases during Li deinsertion and insertion.[17,18]

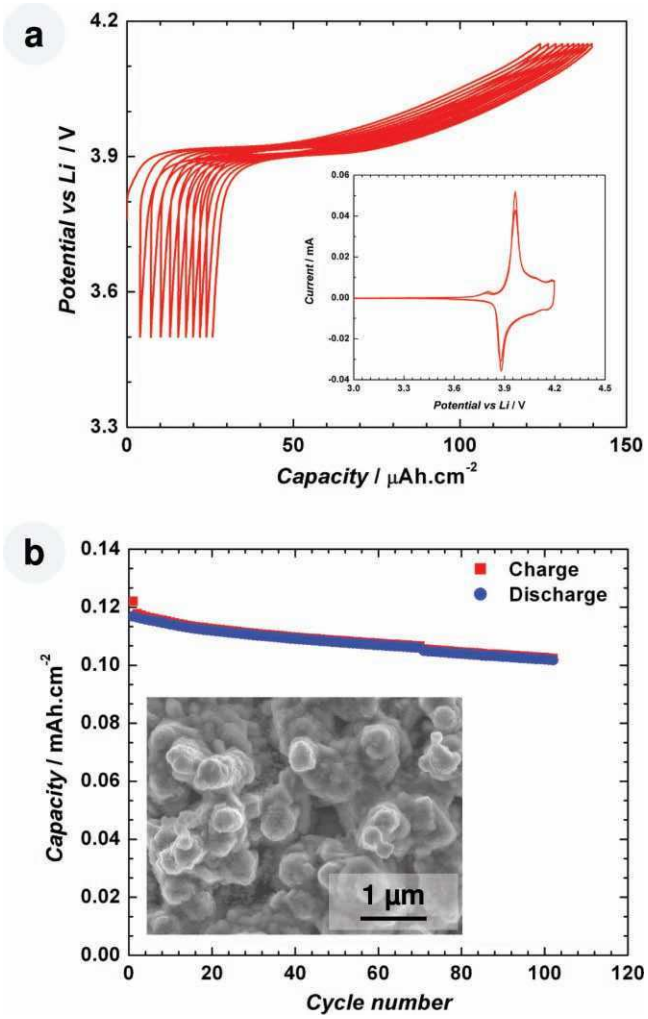

Figure 3. a) Charge–discharge galvanostatic curves for aluminium nanorod-supported $LiCoO_2$ 3D electrode cycled at a rate of *C*/10 versus Li and using a charge cut off voltage of 4.15 V. Inset: cyclic voltamogram of aluminium nanorod-supported $LiCoO_2$ 3D electrode for the initial two cycles at a scan rate of 0.01 mV s^{-1}. b) Capacity retention of the same electrode at a rate of *C*/5. Inset: SEM image of aluminium nanorod-supported $LiCoO_2$ 3D electrode cycled 50 times at *C*/5 rate.

Cyclic voltammetry measurements were performed to measure the reversibility of the nanostructured 3D cathodes by scanning from a potential of 3 V to an upper limit of 4.15 V versus Li at a scan rate of 0.01 mV s^{-1}. The first two voltamograms for Al nanorods-supported $LiCoO_2$ 3D electrode (Figure 3a, inset) were found to be identical. From the cyclic voltamograms (CVs), it can be seen that two sets (cathodic, anodic) of current peaks appeared around the potentials (*V* versus Li) of (3.88 V, 3.94 V), (4.04 V, 4.08 V) and the shapes of the curves are similar to that obtained for bulk $LiCoO_2$, as reported by other research groups.[15] The first set is due to the first-order phase transition between two hexagonal phases (also due to lithium ion de-insertion/insertion process), while the second peaks are caused by the order-disorder phase transition.[17,18] The electrodes were subsequently cycled at a rate of *C*/5 with a charge cutoff voltage of 4.15 V versus Li. The cycling shows negligible hysteresis and the electrodes were found to exhibit excellent capacity retention as shown in Figure 3b. This reflects good stability of the $LiCoO_2$ deposit onto 3D Al nanorods over repeated cycling, showing negligible structural deformation (Figure 3b, inset).

Al nanorods-supported $LiCoO_2$ 3D positive electrodes were tested for their rate capability according to a common protocol, signature curves.[19] Signature curves were collected on discharge using a cut off potential of 3.5 V, after the cells were charged to 4.15 V at a very low current rate (*C*/20). Signature curves were performed after the first 4 cycles of charge–discharge, to determine the full cell capacity (*Q*). **Figure 4** shows the variation of cell capacity as a function of the applied rate expressed in terms of *C*, with *C* being defined as the full use of capacity (*Q*) in 1 h. To compare the electrochemical performance of our 3D cathodes with their 2D counterparts, $LiCoO_2$ was deposited onto planar Al substrates (1.32 cm^2, 0.1 mm thick) following the same procedure. 2D planar cathodes with varying film thickness (active electrode mass) were obtained with 2 to 5 layers of $LiCoO_2$ deposition. Bulk $LiCoO_2$ powder was also prepared by thermal decomposition of the sol-gel precursor at 650 °C in air. Electrochemical measurements were made on Li half cells using either 3 or 5 layers of $LiCoO_2$ deposits on a planar Al foil. The electrode geometrical area has been fixed to be 1.32 cm^2 for all the electrodes studied. With the same electrode deposition conditions, the nanostructured 3D electrode shows more than a twofold improvement in areal capacity compared to its 2D counterpart. With the calculated area gain,[7] we expect an ≈10-fold increase in areal capacity; however, we believe that the nanorods current collector is not completely covered with the active material using spray-assisted sol-gel deposition technique. To better compare the rate performance of nanostructured 3D electrode, we studied a thicker (5 layer, ≈1.5 μm thick from SEM observation) $LiCoO_2$ film on a planar Al substrate. With larger active material for the thick 2D film, we observed an increase in the areal capacity close to that of nanostructured 3D electrode. However, this resulted in further lowering of the power capability of the 2D electrode, owing to slower interfacial kinetics and ohmic losses associated with long Li-transport distances. Excellent rate capability is observed for the nanostructured 3D electrodes compared to their planar counterparts and is shown to recover ≈70% of its total capacity at a high rate of 8*C*. This clearly implies that Al nanorods-supported $LiCoO_2$ 3D electrodes exhibit high power density without compromising on their energy density, unlike their 2D counterparts. These experimental results confirm previous calculations showing that such nano-architectured design offers higher capacity per surface unit than conventional planar 2D electrodes.[7,20] As proposed,[6] the present study highlights the necessity for the 3D matrix of electrodes to meet both the requirements of short transport lengths and large energy capacity. Improvements in energy per unit area and high-rate discharge capabilities are the benefits that may be realized for these 3D electrodes. It is possible to further improve the energy density of 3D cathodes by growing longer electrodes, without sacrificing their power capabilities, since the ohmic losses will be negligible for such a 3D design.

To conclude, making a 3D positive electrode with lithium containing active material has been realized for the first time. Al nanorods current collectors were directly electrodeposited

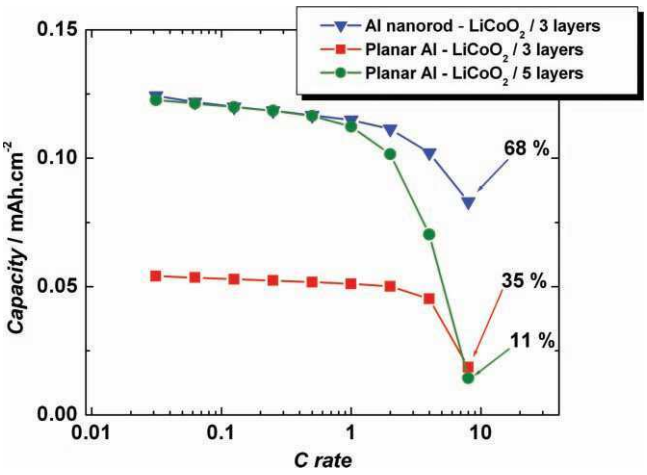

Figure 4. Rate capability plots for Al nanorod-supported $LiCoO_2$ 3D electrode. $LiCoO_2$ films deposited on planar Al foil with different thicknesses (3 and 5 layers of spray-coating) are also compared.

onto Al conducting substrates via template-assisted growth and nanostructured 3D positive electrodes were fabricated by depositing $LiCoO_2$ via thermal decomposition of sol-gel precursors spray-coated onto these nanorods. The importance for 3D matrix of electrodes to meet both the requirements of short transport lengths (power capability) and large energy capacities were highlighted using detailed electrochemical studies. Finally, with these 3D cathodes, we move another step closer towards the realization of the ultimate Li-ion 3D microbattery.

Experimental Section

Preparation of Al nanorod current collectors: Nano-architectured Al current collectors were fabricated using the template technique as previously reported.[7] They were prepared by direct electrodeposition of aluminium into the pores of an anodized alumina oxide (AAO) membrane (Anodisc 47, Whatman) placed on top of an Al disk (1.32 cm^2, 0.1 mm thick), which was mechanically polished and cleaned in ethanol. Electrodeposition was carried out in an argon-filled glove box (O_2 and H_2O <1 ppm) using ionic liquid 1-ethyl-3-methylimidazolium chloride/aluminium chloride (1:2 ratio) as the deposition electrolyte. The electrolyte was prepared by slow addition of aluminium chloride (anhydrous powder, 99.99%, Sigma-Aldrich) into 1-ethyl-3-methylimidazolium chloride (Sigma-Aldrich) under continuous stirring. A brownish liquid was formed at the end of the mixing. Al nanorods were directly synthesized, using pulsed-potential conditions (–0.6 V for 4 ms and –0.35 V for 16 ms) in a three-electrode set up connected to a VMP3 multichannel potentiostat/galvanostat (Bio-logic) unit. Al foil (2 cm by 2 cm) was used as the counter electrode and an Al wire served as the reference electrode. A thick fiberglass separator (Whatman) was soaked with electrolyte and the resulting two-electrode stack was kept under constant pressure by using two stainless-steel clamps during the deposition process. Free standing arrays of aluminium nanorods were obtained after dissolution of the alumina template in an aqueous solution of CrO_3 (1.8 wt%) and H_3PO_4 (6 wt%).[7]

Preparation of Al nanorod-supported $LiCoO_2$ 3D electrodes: For the preparation of nanostructured $LiCoO_2$, a stoichiometric amount of nitrate salts (Li:Co = 1:1) was dissolved in deionized water and thoroughly mixed with ethylene glycol and citric acid (1:4 molar ratio) and then evaporated at 80 °C for 6 h to form transparent sol.[14] The sol was spray-coated onto the Al nanorods arrays to uniformly cover the surface, followed by drying in air at 60 °C for 1 h. The substrate surface was carefully wiped again to remove the salts crystallized on the surface and heated at 650 °C for 8 h in air atmosphere. The entire process was repeated 3–5 times for each sample, resulting in the formation of thick standard coating of nanostructured $LiCoO_2$ onto the Al nanorods arrays. The $LiCoO_2$ coating thickness was estimated to be 30 nm from TEM images.

Characterization of 3D positive electrodes: The microstructure and surface morphology of 3D electrodes were characterized by X-ray diffraction (Bruker AXS D4 Endeavor, Cu Kα), field emission scanning electron microscopy (JEOL JSM 6700F), and transmission electron microscopy (JEOL JEM 2100F). Electrochemical characterizations were performed using VMP3 multichannel potentiostat/galvanostat (Bio-logic). Coin-type cells were assembled in an argon-filled glove box (MBRAUN Unilab) using $LiCoO_2$ active material self supported on Al nanorods as the positive electrode and Li metal as the negative electrode. Both positive and negative electrodes were electronically separated by a Whatman GF/D borosilicate fibreglass sheet soaked with 1 M $LiPF_6$ electrolyte solution (in EC:DMC/1:1 in mass ratio) from Merck.

Acknowledgements

The authors are thankful to Pascal Lenormand and Lucien Datas for their help in SEM and TEM imaging of the samples. This work is supported by SUPERLION within EU-FP7 as well as by the ALISTORE-ERI (Fédération de Recherche CNRS #3104).

[1] J.-M. Tarascon, M. Armand, *Nature* **2001**, *414*, 359.
[2] P. G. Bruce, B. Scrosati, J.-M. Tarascon, *Angew. Chem. Int. Ed.* **2008**, *47*, 2930.
[3] B. L. Ellis, K. T. Lee, L. F. Nazar, *Chem. Mater.* **2010**, *22*, 691.
[4] P.-L. Taberna, S. Mitra, P. Poizot, P. Simon, J.-M. Tarascon, *Nat. Mater.* **2006**, *5*, 567.
[5] P. Poizot, S. Laruelle, S. Grugeon, L. Dupont, J.-M. Tarascon, *Nature* **2000**, *407*, 496.
[6] J. W. Long, B. Dunn, D. R. Rolison, H. S. White, *Chem. Rev.* **2004**, *104*, 4463.
[7] E. Perre, L. Nyholm, T. Gustafsson, P.-L. Taberna, P. Simon, K. Edström, *Electrochem. Commun.* **2008**, *10*, 1467.
[8] S. K. Cheah, E. Perre, M. Rooth, M. Fondell, A. Hårsta, L. Nyholm, M. Boman, T. Gustafsson, J. Lu, P. Simon, K. Edström, *Nano Lett.* **2009**, *9*, 3230.
[9] D. Golodnitsky, M. Nathan, V. Yufit, E. Strauss, K. Freedman, L. Burstein, A. Gladkich, E. Peled, *Solid State Ionics* **2006**, *177*, 2811.
[10] H.-S. Min, B. Y. Park, L. Taherabadi, C. Wang, Y. Yeh, R. Zaouk, M. R. Madou, B. Dunn, *J. Power Sources* **2008**, *178*, 795.
[11] G. F. Ortiz, I. Hanzu, P. Lavela, P. Knauth, J. L. Tirado, T. Djenizian, *Chem. Mater.* **2010**, *22*, 1926.
[12] K. Mizushima, P. C. Jones, Pal. Wiseman, J. B. Goodehough, *Mater. Res. Bull.* **1980**, *17*, 783.
[13] M. S. Whittingham, *Chem. Rev.* **2004**, *104*, 4271.
[14] X. Li, F. Cheng, B. Guo, J. Chen, *J. Phys. Chem.* **2005**, *B109*, 14017.
[15] Y. Gu, D. Chen, X. Jiao, *J. Phys. Chem.* **2005**, *B09*, 17901.
[16] G. Ceder, Y.-M. Chiang, D. R. Sadoway, M. K. Aydinol, Y.-I. Jang, B. Huang, *Nature* **1998**, *392*, 694.
[17] J. N. Reimers, J. R. Dahn, *J. Electrochem. Soc.* **1992**, *139*, 2091.
[18] J. B. Bates, N. J. Dudney, B. J. Neudecker, F. X. Hart, H. P. Jun, S. A. Hackney, *J. Electrochem. Soc.* **2000**, *147*, 59.
[19] M. Doyle, J. Newman, J. Reimers, *J. Power Sources* **1994**, *52*, 211.
[20] S. Grugeon, S. Laruelle, L. Dupont, F. Chevallier, P.-L. Taberna, P. Simon, L. Gireaud, S. Lascaud, E. Vidal, B. Yrieix, J.-M. Tarascon, *Chem. Mater.* **2005**, *17*, 5041.